Insight into the Mechanism of the Thermal Reduction of Graphite Oxide: Deuterium-Labeled Graphite Oxide Is the Key

Zdeněk Sofer,*,† Ondřej Jankovský,† Petr Šimek,† David Sedmidubský,† Jiří Šturala,‡ Jiří Kosina,§ Romana Mikšová,∥,⊥ Anna Macková,∥,⊥ Martin Mikulics,#,∞ and Martin Pumera*,▽

†Department of Inorganic Chemistry, ‡Department of Organic Chemistry, and §Central Laboratories, University of Chemistry and Technology Prague, Technická 5, 166 28 Prague 6, Czech Republic, ∥Department of Neutron Physics, Nuclear Physics Institute of the Academy of Sciences of the Czech Republic, v. v. i., Řež 130, 250 68 Řež, Czech Republic, ⊥Department of Physics, Faculty of Science, J.E. Purkyně University, Ceske mladeze 8, 400 96 Usti nad Labem, Czech Republic, #Peter Grünberg Institute (PGI-9), Forschungszentrum Jülich, 52425 Jülich, Germany, ∞Jülich-Aachen Research Alliance, Fundamentals of Future Information Technology (JARA-FIT), 52425 Jülich, Germany, and ▽Division of Chemistry & Biological Chemistry, School of Physical and Mathematical Sciences, Nanyang Technological University, 21 Nanyang Link, Singapore 637371, Singapore

ABSTRACT For the past decade, researchers have been trying to understand the mechanism of the thermal reduction of graphite oxide. Because deuterium is widely used as a marker in various organic reactions, we wondered if deuterium-labeled graphite oxide could be the key to fully understand this mechanism. Graphite oxides were prepared by the Hofmann, Hummers, Staudenmaier, and Brodie methods, and a deuterium-labeled analogue was synthesized by the Hofmann method. All graphite oxides were analyzed not only using the traditional techniques but also by gas chromatography—mass spectrometry (GC-MS) during exfoliation in hydrogen and nitrogen atmospheres. GC-MS enabled us to compare differences between the chemical compositions of the organic exfoliation products formed during the thermal reduction of these graphite oxides. Nuclear analytical methods (Rutherford backscattering spectroscopy, elastic recoil detection analysis) were used to calculate the concentrations of light elements, including the ratio of hydrogen to deuterium. Combining all of these results we were able to determine graphite oxide's thermal reduction mechanism. Carbon dioxide, carbon monoxide, and water are formed from the thermal reduction of graphite oxide. This process is also accompanied by various radical reactions that lead to the formation of a large amount of carcinogenic volatile organic compounds, and this will have major safety implications for the mass production of graphene.

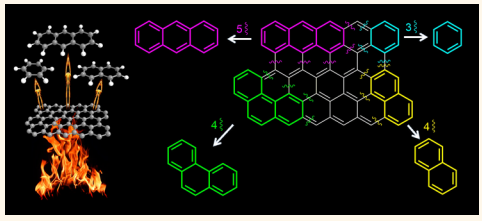

KEYWORDS: graphene · exfoliation · mechanism · isotope labeling · graphite oxide

Graphene, a one-atom-thick planar sheet of sp^2-bonded carbon atoms, has been intensively studied in the past decade due to its unique electrical, optical, and mechanical properties, in particular its low thermal conductivity, high current density, large surface area, high transmittance in the visible light spectrum, and ability to ballistically transport free carriers.[1−3] These unique properties make graphene a highly promising material for a wide range of applications in modern electronics (solar cells, display devices, *etc.*) and electrochemical power sources (fuel cells, supercapacitors, batteries, *etc.*).[4−7]

Graphene is usually synthesized by either "bottom-up" or "top-down" procedures. The "bottom-up" procedures, used for the production of high-quality and large-size graphene layers, are typically based on CVD techniques. These CVD-based graphene layers are important for microelectronic and optoelectronic devices. However, for applications in the field of electrochemical power sources, graphene has to be produced in much larger quantities.[8−10] For this purpose, graphene is prepared using "top-down" methods, of which the most common is the oxidation of graphite and subsequent reduction of graphite oxide.[11] Compared with chemical or electrochemical reduction, the thermal reduction of graphite oxide produces graphene with the highest degree of exfoliation and largest surface area.

* Address correspondence to zdenek.sofer@vscht.cz, pumera@ntu.edu.sg.

Received for review March 8, 2015 and accepted April 20, 2015.

Published online April 20, 2015
10.1021/acsnano.5b01463

The thermal reduction of graphite oxide is generally described as a process of the decomposition of oxygen functional groups in association with the formation of carbon dioxide, carbon monoxide, and water. However, a few papers have suggested that the process is more complex than is generally assumed. One study reported that carbon fragments are released from graphite oxide during thermal exfoliation.[12,13] Another study addressed exfoliation in a closed system, namely, an autoclave in which evolved gaseous species can readily combine with each other. The latter study, which involved the use of gas chromatography−mass spectrometry (GC-MS), detected a larger number of organic compounds, including several carcinogenic compounds, such as benzene and even higher polyaromatic hydrocarbons (PAHs).[14] This seems to indicate that the precise mechanism of the thermal reduction and subsequent exfoliation of graphite oxide has yet to be described in detail.

In this study, GC-MS was used to analyze and quantify various organic compounds formed from the thermal reduction of graphite oxides, including a deuterium-labeled graphite oxide, in a nitrogen or hydrogen atmosphere. Combining the results of the analytical methods used with quantum-mechanic calculations enables us to propose the mechanism of the decomposition of various oxygen functionalities and to clarify the overall exfoliation process.

RESULTS AND DISCUSSION

Four graphite oxides (GOs) were prepared by the Brodie,[15] Hummers,[16] Hofmann,[17] and Staudenmaier[18] methods, and a deuterium-labeled analogue was synthesized according to the Hofmann method by hydrogen/deuterium exchange in deuterium oxide. All samples were further exfoliated in either a nitrogen or hydrogen atmosphere. Below, the samples are termed according to their GO precursor (BR, Brodie; HU, Hummers; HO, Hofmann; ST, Staudenmaier) and the exfoliation atmosphere (N_2 or H_2); the deuterated sample carries the additional suffix De. All samples were then analyzed by scanning electron microscopy (SEM), energy-dispersive spectroscopy (SEM-EDS), combustion elemental analysis, high-resolution X-ray photoelectron spectroscopy (XPS), and Raman spectroscopy. GC-MS was used to analyze the exfoliation products. In addition, the nuclear analytical methods, Rutherford backscattering spectroscopy (RBS) and elastic recoil detection analysis (ERDA), were used to measure the D/H ratio and concentration of light elements. To confirm our experimental results, the decomposition energies of various oxygen functional groups were also calculated. For more details, see the Experimental Methods and Supporting Information (SI).

The morphology and elemental composition of thermally reduced graphene were investigated by SEM and SEM-EDS. The typical platelet structure was observed for all samples; however, the graphene synthesis in hydrogen led to a higher degree of exfoliation compared with the samples exfoliated in nitrogen (Figure 1).

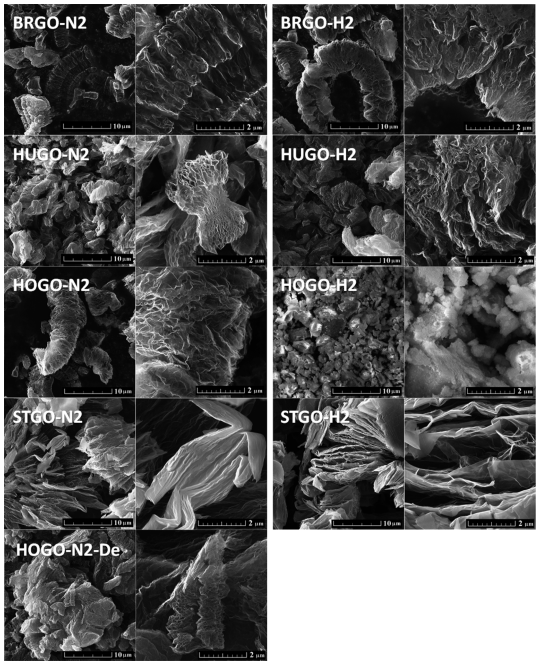

Figure 1. Morphology of all thermally reduced/exfoliated graphenes.

TABLE 1. C/O Ratios (at. %) in Thermally Reduced/Exfoliated Graphite Oxides Obtained from Various Methods

sample	C/O CHN-O	C/O XPS
BRGO-N2	17.6	19.4
BRGO-H2	20.9	24.1
HUGO-N2	22.9	26.0
HUGO-H2	27.5	42.5
HOGO-N2	14.4	18.2
HOGO-H2	30.6	19.8
STGO-N2	20.4	34.7
STGO-H2	20.9	46.6
HOGO-N2-De	18.9	24.7

The chemical composition was studied by SEM-EDS, combustible elemental analysis, and high-resolution X-ray photoelectron spectroscopy. Except for C and O, low concentrations of K, Mn, S, and Cl (0.1 wt %) were detected by SEM-EDS and combustible elemental analysis, respectively. The calculated C/O ratios based on the data from these methods are summarized in Table 1. The results of combustible elemental analysis are presented in detail in Table SI-A. The element distribution maps obtained by SEM-EDS as well as the XPS survey spectra are shown in Figures SI-1 and SI-2, respectively. Exfoliation in a hydrogen atmosphere led to higher reduction of graphene when compared to exfoliation in a N_2 atmosphere, and the highest C/O ratio was obtained for STGO-H2.

TABLE 2. Quantitative Comparison (at. %) of Individual Carbon States of C 1s in Thermally Reduced/Exfoliated Graphite Oxides Obtained by High-Resolution XPS

sample	C=C	C−C/C−H	C−O	C=O	O−C=O	π=π*
BRGO-N2	60.30	18.58	10.16	2.10	4.40	4.43
BRGO-H2	61.70	19.75	2.11	4.08	4.82	7.52
HUGO-N2	69.09	11.53	5.37	3.34	5.38	5.25
HUGO-H2	73.43	11.25	4.04	3.91	3.21	4.14
HOGO-N2	64.99	10.48	9.49	5.38	3.83	5.81
HOGO-H2	54.61	24.28	10.18	5.27	2.60	3.04
STGO-N2	62.12	21.10	3.22	3.87	2.53	7.13
STGO-H2	70.26	16.19	2.60	3.31	2.15	5.46
HOGO-N2-De	55.29	20.15	12.34	3.85	4.28	4.06

TABLE 3. D/G Ratios and the Corresponding Crystallite Sizes of the Thermally Exfoliated/Reduced Graphite Oxides Measured by Raman Spectroscopy

sample	D/G ratio	L_a (nm)
BRGO-N2	0.95	20.24
BRGO-H2	0.97	19.81
HUGO-N2	0.98	19.56
HUGO-H2	0.86	22.25
HOGO-N2	0.80	24.00
HOGO-H2	0.82	23.41
STGO-N2	0.74	25.93
STGO-H2	0.83	23.20
HOGO-N2-De	0.92	20.91

In addition, high-resolution XPS was also used for the detailed analysis of the C 1s to quantitatively differentiate the six different carbon states present in all samples: C−C (284.4 eV); C−C/C−H (285.4 eV); C−O (286.3 eV); C=O (288.0 eV); O−C=O (289.0 eV); and $\pi-\pi^*$ interaction (290.5 eV). The quantitative compositions of the individual states of C 1s are listed in Table 2, while the detailed fitting of the C 1s peak is shown in Figure SI-3.

Raman spectroscopy was used to obtain more information about the structure of the synthesized graphenes (Figure SI-4). Two major bands corresponding to the D-band (1350 cm^{-1}) and G-band (1580 cm^{-1}) were found in all spectra.[19] The presence of the D-band indicates defects in the graphene layer, primarily attributable to the presence of sp^3-bonded carbon atoms. The G-band resulted from sp^2-bonded carbon atoms in the graphene layer.[20] Furthermore, the average crystallite size (L_a) of the defect-free domains within the graphene was calculated using the equation[21]

$$L_a = 2.4 \times 10^{-10} \times \lambda_{laser}{}^4 \times I_G/I_D \qquad (1)$$

where I_G/I_D is the ratio of the intensities of the D- and G-bands, respectively, and λ_{laser} refers to the laser wavelength (nm) used in the measurement of the Raman spectrum. The calculated D/G ratios and the corresponding crystallite sizes are compiled in Table 3. The D/G ratio is lowest for samples originating from STGO due to the low content of oxygen functionalities. Higher D/G was observed for HOGO followed by HUGO and finally BRGO. This clearly indicates a significant influence of graphite oxide preparation method on graphene structure and defect density. A slightly higher D/G ratio observed for samples exfoliated in hydrogen (except the HUGO sample) compared to nitrogen originates from graphene etching by hydrogen at high temperature.

GC-MS of exfoliation products of the individual graphite oxides was carried out in different atmospheres. The results of GC-MS analysis of gases evolved during exfoliation of various graphite oxides are shown in Figure 2A for graphite oxides exfoliated in a nitrogen atmosphere and in Figure 2B for graphite oxides exfoliated in a hydrogen atmosphere. The detailed GC-MS data for each sample are shown in the SI (Figures SI-5−SI-12). Also the logarithmic scale of each GC-MS spectrum is shown in the SI with illustrations of formed products. Structures of the main products of exfoliation are visualized in Figure 2C. To understand more deeply the processes occurring during thermal exfoliation of graphite oxide, we performed a careful analysis and quantification of the formed organic compounds. Deuterium-labeled HOGO (HOGO-De) was used to understand the mechanism of acidic oxygen functionalities' thermal decomposition. The experimental results are supported by theoretical calculations.

The main differences in the composition of gaseous products released during exfoliation can be seen for the graphite oxide prepared by the Brodie method. The Brodie oxidation procedure is based on the oxidation of graphite by potassium chlorate in fuming nitric acid. In this case we did not observe any significant amount of exfoliation products related to sulfur incorporated into the graphite oxide by the oxidation procedure. All other methods (Hummers, Hofmann, and Staudenmaier), which also use sulfuric acid in addition to HNO_3, led to the graphite oxide containing sulfur, mainly in the form of sulfuric acid esters, which decompose into sulfur dioxide during thermal exfoliation. This observation led us to a conclusion that sulfuric acid is dominantly present in the graphite oxide as an ester of sulfuric acid bonded by one or both hydroxyl groups to the hydroxyl group on the surface of graphite oxide.[22,23] However, also carbon disulfide and some organic compounds of sulfur such as thiophene, benzothiophene, and dibenzothiophene were detected in exfoliation products. This indicates that during the exfoliation highly reactive radicals containing carbon were also formed, and they subsequently reacted with SO_2 during the exfoliation procedure. However, CS_2 was not formed during exfoliation in a hydrogen atmosphere, and also the amount of SO_2 was

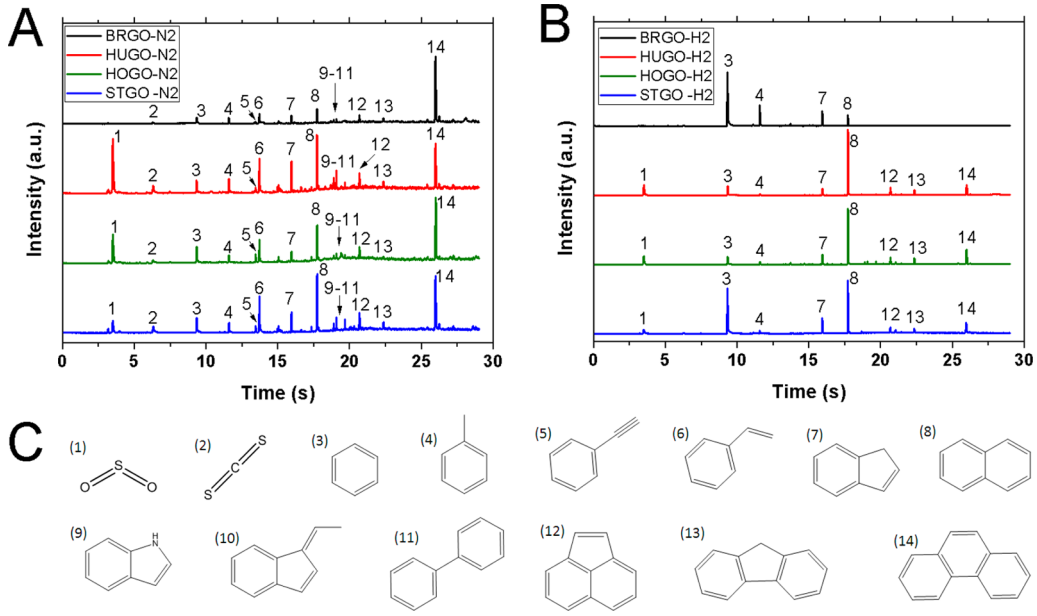

Figure 2. GC-MS chromatogram of compounds evolved during graphite oxide reduction/exfoliation in nitrogen (A) and hydrogen (B) atmospheres and the main formed products (C). Detailed chromatograms with *y*-axes in log scale are shown in the SI.

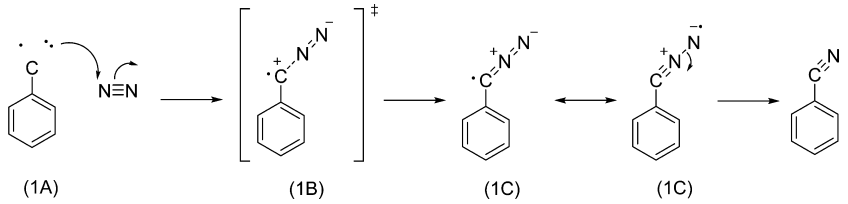

Scheme 1. Mechanism of benzonitrile formation with intermediate states.

significantly reduced. This brings us to a conclusion that H_2S is likely formed as a dominant product in the hydrogen atmosphere reducing environment, although it was not detected on the SPME fiber used for sorption sampling of evolved gases.

Chlorine present in the graphite oxide is evolved in the form of chlorobenzene and nitrogen in the form of nitrile groups attached to hydrocarbons such as 2-propenenitrile and benzonitrile. This is another indication that the radical reactions play a significant role during the exfoliation of graphite oxide. Nitrogen derivates can be formed by the reaction with nitrogen from the atmosphere and also from traces of nitrogen covalently bonded to graphite oxide. The latter mechanism is supported by the fact that these species were also observed in a hydrogen exfoliation atmosphere. Nitrogen in graphite oxide originates from the nitrogen moieties introduced by synthesis of graphite oxide in the presence of nitric acid (or sodium nitrate in the case of the HUGO sample). The radical mechanism of benzonitrile formation can be described by Scheme 1. The fragmentation of the graphene sheet may result in the formation of a relatively stable structure (1A), which may exist in a doublet or quartet spin state. Both of these structures react readily with nitrogen, forming a linear structure (1C) *via* a transient state (1B). Elimination of nitrogen from these structures results in benzonitrile.

Carbon is represented by various aromatic compounds in the GC-MS spectra. During the exfoliation of GO, benzene, toluene, and other derivatives of benzene are dominantly formed. Polyaromatic compounds are represented by naphthalene, its derivates, and higher hydrocarbons such as phenanthrene, anthracene, fluorene, and acenaphthylene. TenaxGR sorption tubes in combination with a specialized GC column allowed the detection of larger polyaromatic compounds such as chrysene. The formation of aromatic hydrocarbons during thermal exfoliation proceeds by a radical mechanism and will be discussed in the next paragraphs.

Further we performed a quantification of the evolved organic molecules. The most striking differences between the treatment in hydrogen and nitrogen atmosphere were observed in the absolute amount of the evolved hydrocarbons. The measurement was performed using active carbon sorption tubes placed behind the exfoliation reactor. In these experiments HUGO and HOGO samples were examined. The detection limit was about 0.1 ppm, referred to the mass of starting graphite oxide. In the case of a

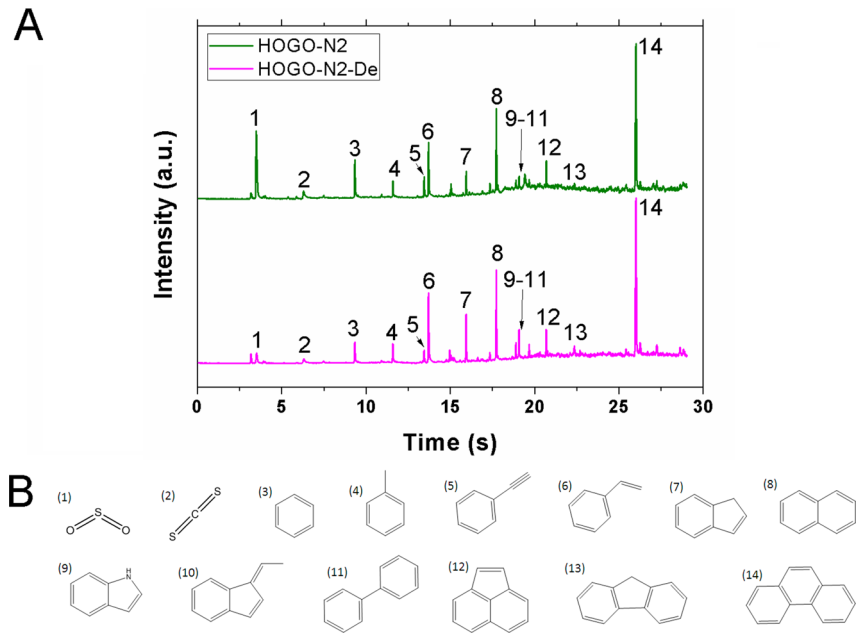

Figure 3. GC-MS chromatogram of compounds evolved during thermal exfoliation/reduction of (A) HOGO and its deuterated analogues and (B) the main formed products. Detailed chromatograms with *y*-axes in log scale are shown in the SI.

nitrogen atmosphere the exfoliation led to the formation of 20 ppm (±1 ppm) of benzene, 10 ppm (±1 ppm) of toluene, and 1 ppm (±0.2 ppm) of naphthalene for both investigated graphite oxides. The concentration of other organic species was below 1 ppm. The amount of evolved organic compounds is almost independent of the used starting graphite oxide. The same process was also performed in the hydrogen atmosphere. In this case the results were significantly different. The exfoliation procedure is accompanied by an intensive etching of the formed graphene. During the exfoliation the formation of 285 ppm (±10 ppm) of benzene, 11 ppm (±1 ppm) of toluene, and 20 ppm (±1 ppm) of naphthalene for both HOGO and HUGO was observed. Such results indicate that hydrogen etching is an important and dominant process during thermal exfoliation of graphite oxide in a reductive atmosphere. This observation is essential for future high-temperature applications of graphene in a reductive atmosphere and also for the production of thermally reduced graphene where high amount of evolved toxic products could have a significant impact on the environment.

In order to understand the exfoliation mechanism, the deuterium-labeled graphite oxide was synthesized. By the ultrasonication and prolonged soaking of graphite oxide in deuterium oxide the acidic hydrogen contained in functional groups (predominantly the carboxylic groups located on the graphite oxide sheet edges) was exchanged with deuterium. Nuclear methods with isotope sensitivity, elastic recoil detection analysis, and Rutherford backscattering spectrometry were used for the determination of D/H ratio.

The RBS and ERDA spectra of deuterated samples are shown in the SI (see Figures SI-13 and SI-14). The

TABLE 4. Composition of HOGO before and after Exfoliation in Nitrogen Atmosphere

sample	C [at. %]	O [at. %]	H [at. %]	D [at. %]
HOGO-N2-De (RBS/ERDA)	83.0	6.3	9.5	1.2
HOGO-N2-De (ECA)	89.55	4.75	5.70	
HOGO-N2 (RBS/ERDA)	83.9	6.5	9.6	0.0
HOGO-N2 (ECA)	88.62	6.14	5.22	
HOGO-De (RBS/ERDA)	64.4	21.6	13.7	0.3
HOGO-De (ECA)	53.12	25.89	20.05	
HOGO (RBS/ERDA)	65.7	22.7	11.1	0.0
HOGO (ECA)	46.65	31.27	22.08	

measurement of deuterium content was performed on the starting HOGO and the deuterium-exchanged material before and after exfoliation in a nitrogen atmosphere. In addition, a GC-MS analysis of the evolved gases was performed. The GC-MS analyses of the evolved gases for samples HOGO-N2 and HOGO-N2-De in a nitrogen atmosphere are shown in Figure 3A. The composition of the starting D-labeled HOGO was 64.4 at. % C, 21.6 at. % O, 13.7 at. % H, and 0.3 at. % D. The concentration of deuterium corresponds to the concentration of carboxylic acid measured by alkalimetric titration. A low concentration of deuterium indicates a highly lipophilic character of the hydroxyl groups where no hydrogen/deuterium exchange takes place. The sample composition after the exfoliation measured by RBS and ERDA was 83.0 at. % C, 6.3 at. % O, 9.5 at. % H, and 1.2 at. % D. The results of RBS/ERDA for HO-GO and HO-GO-De before and after thermal reduction/exfoliation are shown in Figures SI 13 and SI 14, and the results of elemental combustion analysis (ECA) and RBS/ERDA are summarized in Table 4. The results indicate that the

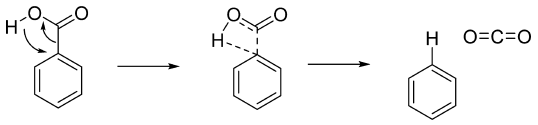

Scheme 2. Schematic drawing of aromatic compound decarboxylation resulting in hydrogenation and CO_2 formation.

combination of RBS and ERDA can be used for effective quantitative analysis of graphene-based materials, and in addition the isotopic ratio for light atoms can be quantified.

The slight differences in the composition of HOGO and HOGO-De obtained by RBS/ERDA and elemental combustion analysis can originate from partial decomposition of graphite oxide under irradiation with high-energy ion beam in an ultra-high-vacuum environment. However, the D/H ratio remains unaffected due to almost identical chemical properties of D and H. The presence of deuterium in the exfoliated sample clearly demonstrates the hydrogenation mechanism on thermal exfoliation of graphite oxide. The carboxylic groups are apparently decomposed into CO_2 and hydrogen (deuterium) radical, which is directly attached to the graphene sheet edge. The schematic diagram for the proposed mechanism is shown in Scheme 2. The *ab initio* calculations were performed in order to see the differences between various carboxylic acid positions on the rim of the graphene sheet. Big differences between the standard Gibbs energies (150−230 kJ/mol) of the starting acid and the corresponding transient state at 1173 K are closely related to the carboxylic acid position within graphene oxide. The lowest energy of thermal decomposition of the COOH functional group was obtained for the middle of the graphene rim, where the COOH group cannot take a coplanar geometry with the graphene sheet. The Gibbs energy for decarboxylation with COOH functional groups in various positions is shown in the SI (see Figure SI 15). This observation can be further used for a controlled thermal decomposition of graphene oxide, where the carboxyl functional groups are located on the edges of graphene oxide sheets.

Another significant difference in the composition of the evolved gases is related to sulfur. A significant reduction of sulfur-based species concentration in the evolved gases was observed for the HOGO-De sample compared to HOGO. This led us to a conclusion that sulfur is dominantly bonded to the graphite oxide sheets in the form of sulfuric acid esters. Long treatment with deuterium oxide led to hydrolysis of sulfuric acid esters and subsequent reduction of sulfur concentration covalently bonded to GO. The concentration of sulfur in HOGO and HOGO-De was 0.34 and 0.20 wt %, respectively. This effect is also documented by a significant lowering of SO_2 concentration in the evolved gaseous exfoliation products (Figure 3). A schematic drawing of proposed sulfuric acid ester decomposition is shown in Scheme 3.

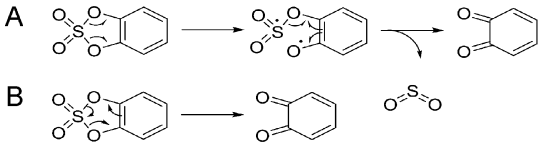

Scheme 3. Schematic drawing of sulfate ester moiety decomposition by a two-step radical mechanism (A) and by a cyclic mechanism (B).

Similar dominant exfoliation products can be observed in the GC-MS chromatographs: benzene, toluene, naphthalene, phenanthrene, and anthracene for all types of starting graphite oxides. Careful analysis of MS spectra for these species showed singly deuterated aromatic hydrocarbons: benzene, toluene, and naphthalene. Surprisingly, no deuterated phenanthrene or anthracene was detected. The MS spectra of single-deuterated benzene and other organic compounds are shown in the SI (see Figure SI 16). This clearly indicates that plucking of aromatic hydrocarbons starts from the graphene sheet edges where the carboxylic functional groups were originally located. The exfoliation procedure led first to decarboxylation with simultaneous hydrogenation and subsequently to the ripening of benzene and other small aromatic molecules, which turned out to be singly deuterium substituted. Further etching of the formed graphene is accompanied by plucking of higher polyaromatic compounds such as phenanthrene. Surprisingly, among higher aromatic compounds phenanthrene is clearly dominating, while only minor amounts of anthracene and heavier polyaromatic compounds were detected. This can be interpreted in terms of lower energy necessary for ripping off the bent aromatic molecules compared to linear ones, where more carbon bonds must be broken off. This is supported by the observation of chrysene and the absence of tetracene in the exfoliation products using a technique more sensitive for highly polyaromatic compounds. The plucking of aromatic ring fragments and their subsequent rearrangement are clearly documented by the presence of molecules such as ethylidene-1*H*-indene, acenaphthylene, styrene, fluorene, indane, and others. The proposed mechanism for various hydrocarbons formation is shown in Scheme 4.

The presence of nitrogen in the form of a nitrile group indicates that the exfoliation and subsequent partial etching of the formed graphene proceed by a radical mechanism. The evolved hydrocarbon fragments are in the form of radicals, and they immediately react with the surrounding atmosphere to form 2-propenenitrile. This compound is released together with other unsaturated hydrocarbons such as but-1-yne and but-1-en-3-yne. Such compounds were not detected in the samples exfoliated in a hydrogen atmosphere due to their high reactivity. However, traces of nitrile-containing compounds such as benzonitrile were

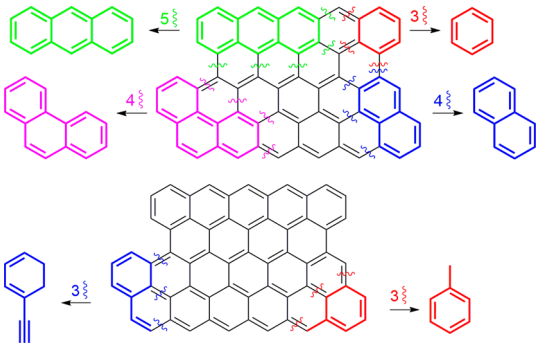

Scheme 4. Mechanism of radical formation of various hydrocarbons during graphite oxide thermal exfoliation. Numbers indicate the amount of bonds that must be broken off. More complex compounds may require some "prearrangement", which is usually achieved by benzene ripping.

observed also for samples exfoliated in a hydrogen atmosphere. Another evidence for the radical mechanism playing a dominant role in the exfoliation procedure is the presence of chlorobenzene, which is formed in the gaseous phase by a reaction of chlorine radical and benzene evolved during exfoliation.

Surprisingly, only a minor amount of oxygen-containing molecules was formed. Most of the oxygen functionalities are decomposed to CO_2 and CO. From the oxygen-containing molecules benzofuran, dibenzofuran, and phenol were detected. Formation of such molecules is challenging to explain. They can originate from both the hydroxyl or epoxide groups on the graphite oxide surface, or they can be formed in the next step by the reaction of evolved water with benzene and ethylbenzene radicals.

Finally we investigated the kinetics of the graphite oxide exfoliation process. For this purpose we performed sampling of the evolved gases in 3 min intervals using SPME fiber. The experiments were performed for HOGO and HUGO in both nitrogen and hydrogen atmospheres. The process of exfoliation proceeds extremely fast, and in the nitrogen atmosphere most volatile organic molecules are evolved during the first minutes when the graphite oxide sample is heated over an exfoliation temperature. Slight differences are observed in the case of the hydrogen atmosphere, where the partial etching of graphene occurs. This is clearly documented by a slower decrease of benzene concentration as well as other aromatic volatile organic species (VOCs). However, the vast majority of VOCs evolved during the first 3 min of the exfoliation procedure in a hydrogen atmosphere. The data are summarized in Figure SI 17 for HUGO and Figure SI 18 for HOGO, where the complete chromatographs for each 3 min sequence are shown, together with detailed data of benzene peak time evolution as an example.

CONCLUSIONS

We have shown that the thermal reduction/exfoliation of graphite oxide leads not only to the formation of simple molecules (carbon dioxide, carbon monoxide, water) but also to many complex organic compounds. This suggests that a radical mechanism is at play during graphite oxide thermal exfoliation. The experimental reduction/exfoliation of deuterium-labeled graphite oxide and theoretical *ab initio* calculations confirmed that the simultaneous hydrogenation of graphene edges and preferential etching of carbon led to the formation of benzene and naphthalene. We successfully quantified the dominant species that evolved during reduction/exfoliation. The exfoliation of 1 kg of graphite oxide led to the formation of over 0.3 g of VOCs, but it was 1 order of magnitude worse in the hydrogen atmosphere, which implies the enhanced etching of graphene edges by hydrogen. Thus, our investigation of the actual mechanism of the thermal reduction/exfoliation of graphite oxide has led us to results that are somewhat alarming. Put simply, the mass production of thermally reduced graphene could have a significant negative impact on the environment due to the formation of highly carcinogenic compounds.

EXPERIMENTAL METHODS

A detailed experimental section can be found in the SI. In the first step we prepared four graphite oxides according to the Brodie, Hummers, Hofmann, and Staudenmaier methods. These graphite oxides were termed BRGO, HUGO, HOGO, and ST-GO. Also deuterium-labeled graphite oxide was prepared according to the Hofmann method by hydrogen/deuterium exchange in deuterium oxide.

The thermal reduction–exfoliation of graphite oxide was performed at 800 °C in a quartz glass reactor. Thermally reduced graphenes were performed in a hydrogen and nitrogen atmosphere, respectively, at 800 °C and a pressure of 100 kPa. Graphite oxide was placed in a porous quartz glass capsule connected to a magnetic manipulator inside a vacuum tight tube furnace with a controlled atmosphere. The application of a magnetic manipulator allowed us to create a temperature gradient of over 1000 °C min^{-1}. The sample was flushed with nitrogen by repeated evacuation of the tube furnace to remove any traces of oxygen. Subsequently the reactor was filled with nitrogen or hydrogen, respectively, and the sample was quickly inserted by magnetic manipulator to the preheated furnace and held in the furnace for 12 min. The flow of hydrogen or nitrogen during the exfoliation procedure was 1000 sccm to remove the byproducts of the exfoliation procedure. The sampling place for the SPME fiber and active carbon sorption tube was placed on the output of the reactor.

The morphology was investigated using scanning electron microscopy. Elemental composition and mapping were performed using energy dispersive spectroscopy. Combustible elemental analysis (CHNS-O) was performed using a PE 2400 Series II CHNS/O analyzer (PerkinElmer, USA). High-resolution X-ray photoelectron spectroscopy was performed using an ESCAProbeP spectrometer (Omicron Nanotechnology Ltd., Germany) with a monochromatic aluminum X-ray radiation source (1486.7 eV). An inVia Raman microscope (Renishaw, England) in backscattering geometry with a CCD detector was

used for Raman spectroscopy. The Rutherford backscattering spectroscopy and elastic recoil detection analysis were performed at a Tandetron 4130 MC tandem accelerator.

The exfoliation in nitrogen or hydrogen and subsequent sampling on the output of the reactor was performed using an SPME (solid-phase microextraction) fiber for qualitative analysis and active carbon sorption tubes for total quantification of evolved organic species. Such a configuration minimizes retention time in the hot zone of the reactor, and immediate cooling of carrier gas allowed preservation of highly reactive species containing also double and triple carbon−carbon bonds. To determine what kind of organic compounds are evolved during exfoliation of GO, gaseous products were sampled on the 85 μm Carboxen/PDMS SPME fiber (Supelco, USA) and analyzed on a gas chromatograph coupled by a mass spectrometer (GC-MS). Prior to sampling, the used SPME fiber was conditioned for 30 min at 240 °C under a constant flow of helium. The conditioned SPME fiber was inserted *via* a Teflon septum into the outline of the reactor cell, and the sample was collected over 12 min. The exposed SPME fiber was thermally desorbed in the heated split/splitless injection port of the GC (Trace GC Ultra, Thermo Scientific, USA) under a constant flow of carrier gas (helium). The flow of helium was set to 1.5 mL/min. The injection port was heated to 240 °C and worked in the split mode. The split ratio was set to a value of 1:10.

Chromatographic separations were performed on a DB-5MS capillary column (Agilent J&W, USA; 60 m × 0.32 mm i.d. and 1.0 μm). The GC oven program was as follows: initial temperature 40 °C, hold for 5 min, 15 °C/min to 250 °C, hold for 10 min. Masses in the range 10 to 400 *m/z* in full scan mode were recorded on the ISQ (Thermo Scientific, USA) single-quadrupole MS operating at an electron impact energy of 70 eV. Acquired mass spectra were interpreted by using the NIST 05 electronic database.

To determine the total amount of evolved organic species, gaseous products were sampled on the ORBO-32 active carbon sorption tube (Supleco, USA) connected directly into the exhaust line of the exfoliation cell. Trapped compounds on the active carbon were extracted by 1 mL of CS_2 (>99.9%, low benzene content, Sigma-Aldrich, Czech Republic) and analyzed by injecting 1 μL of the CS_2 extract into the same GC-MS used for analysis of the exposed SPME fiber operated under the same conditions.

Conflict of Interest: The authors declare no competing financial interest.

Supporting Information Available: Details of experimental procedures; results of elemental combustion analysis; C and O distribution from SEM-EDS; XPS spectra of graphene; Raman spectra of graphene; details of GC-MS chromatographs in linear and logarithmic scale; RBS and ERDA spectra of graphene; calculations of carboxylic acid decomposition energy details of MS spectra; time dependence of exfoliation products' composition obtained by GC-MS. This material is available free of charge *via* the Internet at http://pubs.acs.org.

Acknowledgment. This work was supported by Czech Science Foundation (Project No. 15-09001S) and by Specific University Research (Project No. MSMT 20/2015). The authors also greatly appreciate the access to computing and storage facilities owned by parties and projects contributing to the National Grid Infrastructure MetaCentrum, provided under the program "Projects of Large Infrastructure for Research, Development, and Innovations" (LM2010005). M.P. acknowledges Tier 2 grant (MOE2013-T2-1-056) from Ministry of Education, Singapore. RBS and ERDA analyses were realized at CANAM (Center of Accelerators and Nuclear Analytical Methods) LM 2011019. A.M. and R.M. were supported by the Czech Science Foundation (Project No. P108/12/G108). M.P. and Z.S. designed the research; Z.S., J.K., P.Š., O.J., D.S., M.M., R.M., and A.M. performed the experiments and analyzed the data; J.S. performed theoretical calculations; Z.S., O.J., and M.P. wrote the manuscript.

REFERENCES AND NOTES

1. Zhang, Y.; Tang, T.-T.; Girit, C.; Hao, Z.; Martin, M. C.; Zettl, A.; Crommie, M. F.; Shen, Y. R.; Wang, F. Direct Observation of a Widely Tunable Bandgap in Bilayer Graphene. *Nature* **2009**, *459*, 820–823.
2. Geim, A. K.; Novoselov, K. S. The Rise of Graphene. *Nat. Mater.* **2007**, *6*, 183–191.
3. Katsnelson, M.; Novoselov, K.; Geim, A. Chiral Tunnelling and the Klein Paradox in Graphene. *Nat. Phys.* **2006**, *2*, 620–625.
4. Wang, X.; Zhi, L.; Müllen, K. Transparent, Conductive Graphene Electrodes for Dye-Sensitized Solar Cells. *Nano Lett.* **2008**, *8*, 323–327.
5. Novoselov, K. S.; Fal, V.; Colombo, L.; Gellert, P.; Schwab, M.; Kim, K. A Roadmap for Graphene. *Nature* **2012**, *490*, 192–200.
6. Bonaccorso, F.; Sun, Z.; Hasan, T.; Ferrari, A. Graphene Photonics and Optoelectronics. *Nat. Photonics* **2010**, *4*, 611–622.
7. Yang, N.; Zhai, J.; Wang, D.; Chen, Y.; Jiang, L. Two-Dimensional Graphene Bridges Enhanced Photoinduced Charge Transport in Dye-Sensitized Solar Cells. *ACS Nano* **2010**, *4*, 887–894.
8. Stoller, M. D.; Park, S.; Zhu, Y.; An, J.; Ruoff, R. S. ; Graphene-Based Ultracapacitors. *Nano Lett.* **2008**, *8*, 3498–3502.
9. Liu, C.; Yu, Z.; Neff, D.; Zhamu, A.; Jang, B. Z. Graphene-Based Supercapacitor with an Ultrahigh Energy Density. *Nano Lett.* **2010**, *10*, 4863–4868.
10. Qu, L.; Liu, Y.; Baek, J.-B.; Dai, L. Nitrogen-Doped Graphene as Efficient Metal-Free Electrocatalyst for Oxygen Reduction in Fuel Cells. *ACS Nano* **2010**, *4*, 1321–1326.
11. Gao, W.; Alemany, L. B.; Ci, L.; Ajayan, P. M. New Insights into the Structure and Reduction of Graphite Oxide. *Nat. Chem.* **2009**, *1*, 403–408.
12. Jankovský, O.; Kučková, Š. H.; Pumera, M.; Šimek, P.; Sedmidubský, D.; Sofer, Z. Carbon Fragments are Ripped off from Graphite Oxide Sheets during their Thermal Reduction. *New J. Chem.* **2014**, *38*, 5700–5705.
13. Ambrosi, A.; Wong, G. K. S.; Webster, R. D.; Sofer, Z.; Pumera, M. Carcinogenic Organic Residual Compounds Readsorbed on Thermally Reduced Graphene Materials are Released at Low Temperature. *Chem. Eur. J.* **2013**, *19*, 14446–14450.
14. Sofer, Z.; Simek, P.; Pumera, M. Complex Organic Molecules are Released during Thermal Reduction of Graphite Oxides. *Phys. Chem. Chem. Phys.* **2013**, *15*, 9257–9264.
15. Brodie, B. C. Sur le Poids Atomique du Graphite. *Ann. Chim. Phys.* **1860**, *1860*, 466–472.
16. Hummers, W.; Offeman, R. Preparation of Graphitic Oxide. *J. Am. Chem. Soc.* **1958**, *80*, 1339–1339.
17. Hofmann, U.; Frenzel, A. Die Reduktion von Graphitoxyd mit Schwefelwasserstoff. *Kolloid-Z.* **1934**, *68*, 149–151.
18. Staudenmaier, L. Verfahren zur Darstellung der Graphitsäure. *Ber. Dtsch. Chem. Ges.* **1898**, *31*, 1481–1487.
19. Dreyer, D. R.; Ruoff, R. S.; Bielawski, C. W. From Conception to Realization: An Historial Account of Graphene and Some Perspectives for Its Future. *Angew. Chem., Int. Ed.* **2010**, *49*, 9336–9344.
20. Dresselhaus, M. S.; Jorio, A.; Hofmann, M.; Dresselhaus, G.; Saito, R. Perspectives on Carbon Nanotubes and Graphene Raman Spectroscopy. *Nano Lett.* **2010**, *10*, 751–758.
21. Cancado, L.; Takai, K.; Enoki, T.; Endo, M.; Kim, Y.; Mizusaki, H.; Jorio, A.; Coelho, L.; Magalhaes-Paniago, R.; Pimenta, M. General Equation for the Determination of the Crystallite Size L_a of Nanographite by Raman Spectroscopy. *Appl. Phys. Lett.* **2006**, *88*, 163106–163106-3.
22. Titelman, G.; Gelman, V.; Bron, S.; Khalfin, R.; Cohen, Y.; Bianco-Peled, H. Characteristics and Microstructure of Aqueous Colloidal Dispersions of Graphite Oxide. *Carbon* **2005**, *43*, 641–649.
23. Dreyer, D. R.; Park, S.; Bielawski, C. W.; Ruoff, R. S. The Chemistry of Graphene Oxide. *Chem. Soc. Rev.* **2010**, *39*, 228–240.